Transition Metal Coordination Compounds of Bisamidobispyridyl Ligands

Peter Comba*[a], Wolfgang Goll[a], Bernhard Nuber[a], and Katalin Várnagy[b]

Anorganisch-Chemisches Institut der Universität[a],
Im Neuenheimer Feld 270, D-69120 Heidelberg, Germany
Fax: (internat.) + 49(0)6221/546617;
E-mail: comba@akcomba.oci.uni-heidelberg.de

Department of Chemistry, Lajos Kossuth University[b],
Debrecen, Hungary

Received July 10, 1998

Keywords: Metal ion selectivity / Stability constants / Molecular mechanics / Metal ion extraction / Liquid membranes

The syntheses of *N*,*N*'-bis-[(2-pyridylmethyl)]-1,3-diamidopropane ($papH_2$) and *N*,*N*'-bis-[(2-pyridylmethyl)]-1,3-diamido-2-hexadecylpropane ($C_{16}papH_2$) are reported together with the results of potentiometric titrations of $papH_2$ with Co(II), Ni(II), Cu(II) and Zn(II), spectroscopic and electrochemical data of [Ni(pap)] and [Cu(pap)], structural studies involving the X-ray analyses of the metal-free $papH_2$ ligand and the corresponding Ni(II) and Cu(II) complexes [Ni(pap)] × 2 H_2O and [Cu(pap)] × 3 H_2O, and force-field calculations (MM) of [Co(pap)], [Ni(pap)], [Cu(pap)] and [Zn(pap)] and the corresponding complexes of the ligand with *ortho*-methyl-substituted pyridyl groups (Me_2papH_2); the results of metal ion transport [Co(II), Ni(II), Cu(II) and Fe(II)] from aqueous solutions through $C_{16}papH_2$ containing dichloromethane phases are also given. The extractability with $C_{16}papH_2$ increases along the series Fe(II) < Co(II) < Ni(II) < Cu(II), and this is confirmed by the potentiometric data ($papH_2$, aqueous solutions; $\log\beta_{ML}$[Co(II)] = 1.75; $\log\beta_{MLH-2}$[Ni(II)]=–11.49; $\log\beta_{ML}$[Cu(II)]=3.41; $\log\beta_{MLH-2}$-[Cu(II)] = –4.491; $\log\beta_{ML}$[Zn(II)] = 1.87). The structural data (X-ray and MM) indicate that, due to the *ortho* protons of the pyridyl groups and in dependence of the electronic configuration of the metal center, there is a considerable tetrahedral twist of the central MN_4 chromophores {square planar: θ = 0°; tetrahedral: θ = 90°; [Co(pap)]: θ = 15° (MM); [Ni(pap)]: θ = 16° (X-ray), 16° (MM); [Cu(pap)]: θ = 18° (X-ray), 18° (MM); [Zn(pap)]: θ = 23° (MM)}, and this may be enhanced by *ortho*-methyl substitution of the pyridyl donors {[Co(Me_2pap)]: θ = 20° (MM); [Ni(Me_2pap)]: θ = 20° (MM); [Cu(Me_2pap)]: θ = 24° (MM); [Zn(Me_2pap)]: θ = 31° (MM)}, and thus possibly a decrease in the complex stability of Cu(II) and Ni(II) in favor of Zn(II).

Introduction

Metal-ion selectivity, i.e. the enhanced stability of a coordination compound with a given ligand and a specific metal ion, relative to that with other metal ions, may be traced back to electronic effects and the coordination geometry, partly enforced by the ligand system. Donor-atom−metal-ion orbital overlap, the HSAB concept, and ligand field effects describe contributions to the electronic terms, and for hexacoordinate compounds these contribute to the well-known pattern of the *Irving-Williams* series[1]. The steric contributions based on the ligand structure include the reorganization of the most stable conformation of the metal-free ligand to that observed in the coordination compound (unfavorable enthalpy and entropy effects) and steric strain imposed by the metal ion on the ligand and vice versa. Thus, highly preorganized systems, which in the original definition[2] are by necessity relatively rigid ligands which, in the conformation observed in the metal complex, are relatively strain free, lead to comparably high complex stabilities. These properties include the metal ion's preference for a particular metal-ligand distance and for a particular angular distribution of the donor atoms, and they are therefore metal-ion dependent. Hence, molecular mechanics was supposed to be a powerful tool for predicting the steric contribution to metal ion selectivities[3]. There are many reasons why, in reality, this is not necessarily correct[4] but for specific applications encouraging results may be obtained[3][4][5].

Our aim was to develop a type of ligand with the following properties: (i) it should generally lead to relatively high complex stabilities with Co(II), Ni(II), Cu(II) and Zn(II); (ii) substitution of the ligand backbone should lead to a predictable variation of the coordination geometry, with the aim of tuning the metal-ion selectivity by modification of the coordination geometry; (iii) derivatives with a similar complexation behavior should be available for quantitative investigations in aqueous solution and for metal ion extractions into organic phases. *N*,*N*′-bis[(2-pyridylmethyl)]-1,3-diamidopropane ($papH_2$, see formula scheme) fulfills these requirements: Tetradentate ligands with amide and pyridyl donors are appropriate complexing agents for divalent metal ions[6]; the substituted diamidopropane fragment is rather rigid, the hexadecane-substituted ligand *N*,*N*′-bis[(2-pyridylmethyl)]-1,3-diamido-2-hexadecylpropane, $C_{16}papH_2$, is easily accessible and leads to a hydrophobic ligand and complexes that are soluble in organic phases; the *ortho*-protons of the pyridyl groups of tetradentate ligands with *cis*-disposed pyridyl groups enforce a tetrahedral twist from square-planar geometry[7] and lead therefore to a steric destabilization of complexes with electronic preferences of the

  1434−1948/98/1212−2041 $ 17.50+.50/0

metal center for square-planar coordination geometry; derivatives with *ortho*-substituted pyridyl groups (e.g. Me_2-papH_2, see formula scheme) should enhance this effect and thus lead to an increased preference for Zn(II) with respect to Ni(II) and Cu(II).

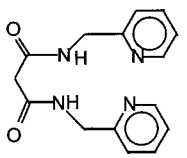

papH$_2$

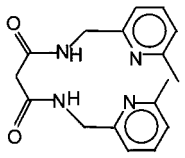

Me$_2$papH$_2$

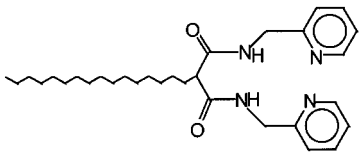

C$_{16}$papH$_2$

Results and Discussion

Syntheses, Spectroscopy and Electrochemistry

C_{16}papH_2 was prepared by alkylation of diethyl malonate with hexadecyl bromide in presence of CH_3CH_2ONa, and subsequent nucleophilic substitution of the alkylated malonic ester with α-picolylamine (Scheme 1); papH_2 was obtained in a similar reaction. Cu(II) and Ni(II) compounds of papH_2 were isolated from aqueous solutions of the metal-free ligands and the metal sulfate salts, or from methanolic solutions and the corresponding tetrafluoroborates; X-ray quality crystals were obtained by slow evaporation of the complex solutions. Spectroscopic and electrochemical parameters of the compounds are listed in Table 1.

Structures

papH$_2$·HBF$_4$ ·H$_2$O: The metal-free ligand crystallizes with a molecule of H_3O^+ BF_4^- in the lattice, and hydrogen bonds are formed between the H_3O^+ ion and the nitrogen atoms of the amide group (2.64 Å). An ORTEP[8] plot of the ligand molecule appears in Figure 1a, and structural

Scheme 1

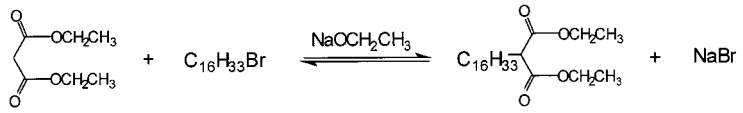

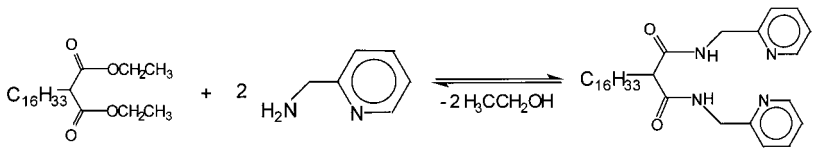

Table 1. Spectroscopic and electrochemical data of [M(pap)]

	UV/Vis		EPR[a]	E[b] [V]
	λ_{max} [nm]	ε [dm^3 mol^{-1} cm^{-1}]		
[Cu(pap)]	571	98	g_{iso} = 2.07 $g_\perp$ = 2.01 $g_{\|\|}$ = 2.19 A_{iso} = 70 × 10^{-4} cm^{-1} $A_\perp$ = 10 × 10^{-4} cm^{-1} $A_{\|\|}$ = 198 × 10^{-4} cm^{-1}	0.10 (Cu$^{II/III}$) 0.23 (Cu$^{I/II}$)
[Ni(pap)]	475	125.5		−1.77 (Ni$^{II/III}$) 0.91 (Ni$^{I/II}$)

[a] From simulation of the experimental spectra. – [b] vs SHE; Cu$^{II/I}$ quasi rev.; Cu$^{III/II}$ irrev.; Ni$^{II/I}$ irrev.; Ni$^{III/II}$ rev.

parameters are listed in Table 2. Bond distances and valence and torsional angles are as expected and similar to those of the coordinated ligand. The geometry around the amide nitrogen and carbon atoms is planar, with little deviation of the corresponding valence angles from 120°. The main differences with respect to the coordinated ligand are: (i) a significantly longer $N_{amide}-C_{amide}$ bond (1.345 Å vs. 1.315 Å); (ii) a smaller $C_{amide}-C_{methylene}-C_{amide}$ valence angle (112° vs. 122° [Ni(II)], 125° [Cu(II)]); (iii) a slightly larger torsion around the $C_{pyridine}-C_{methylene}$ bond (17° vs. 2−10°); (iv) significant changes in the torsion around the $N_{amide}-C_{methylene}$ bond (80° vs. 180°), and (v) significant changes of the torsion around the $C_{amide}-C_{methylene}$ bond (125° vs. 7−18°).

[Cu(pap)] × 3 H_2O: The geometry of the Cu(II) compound is shown in Figure 1b, and the relevant structural parameters are presented, together with those of the Ni(II) compound, in Table 3. An oxygen atom of a neighboring Cu(II) complex molecule is coordinated in an axial position (Cu−O = 2.79 Å). There is also a network of hydrogen bonds between the copper complexes. The central four-coordinate chromophore is unlikely to be perturbed by the axial interactions in the present case. The tetrahedral twist of the CuN_4 chromophore is, as expected, slightly larger than that of the nickel(II) compound (θ° = 18.1°), the torsion around the $Cu-N_{pyridine}$ bond is 10−14° and the resulting α-H ··· α-H distance is 2.17 Å. As in the Ni(II) structure, the six-membered chelate ring is approximately flat and coplanar to the plane defined by the amide donors and the metal center. The five-membered chelate rings are essentially planar. There is a considerable asymmetry with respect to the metal-donor distances but on average the $Cu-N_{pyridine}$ and the $Cu-N_{amide}$ distances are as expected from comparable chromophores[9].

Table 2. Structural parameters of $papH_2 \times HBF_4 \times H_2O$ bond lengths (Å)

O(1)−C(9)	1.223 (4)
N(1)−C(7)	1.454 (5)
N(1)−C(9)	1.345 (4)
N(2)−C(4)	1.348 (5)
N(2)−C(6)	1.342 (4)
C(1)−C(2)	1.381 (6)
C(1)−C(6)	1.391 (5)
C(2)−C(3)	1.376 (6)
C(3)−C(4)	1.377 (6)
C(6)−C(7)	1.503 (5)
C(9)−C(10)	1.518 (4)
C(10)−C(9A)	1.518 (4)
valence angles (deg)	
C(7)−N(1)−C(9)	121.5(3)
C(4)−N(2)−C(6)	120.1(3)
C(2)−C(1)−C(6)	120.3(3)
C(1)−C(2)−C(3)	118.7(4)
C(2)−C(3)−C(4)	119.4(4)
N(2)−C(4)−C(3)	121.6(4)
N(2)−C(6)−C(1)	120.0(3)
N(2)−C(6)−C(7)	119.0(3)
C(1)−C(6)−C(7)	120.9(3)
N(1)−C(7)−C(6)	114.5(3)
O(1)−C(9)−N(1)	122.7(3)
O(1)−C(9)−C(10)	122.4(3)
N(1)−C(9)−C(10)	114.9(3)
C(9)−C(10)−C(9)	112.0(4)

Figure 1. ORTEP[8] plots of the experimentally determined structures of (a) $papH_2 \times HBF \times H_2O$ (HBF × H_2O omitted), (b) [Cu(pap)] × 3 H_2O (H_2O omitted) and (c) [Ni(pap)] × H_2O (H_2O omitted).

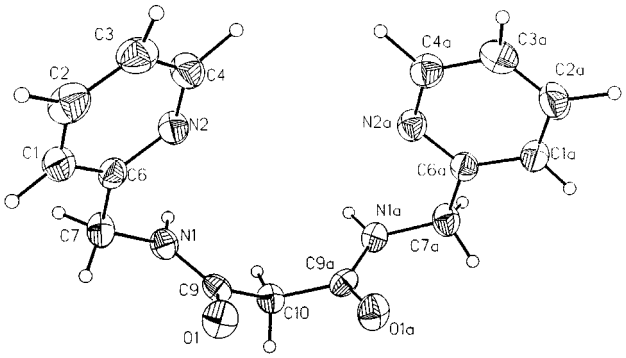

(a)

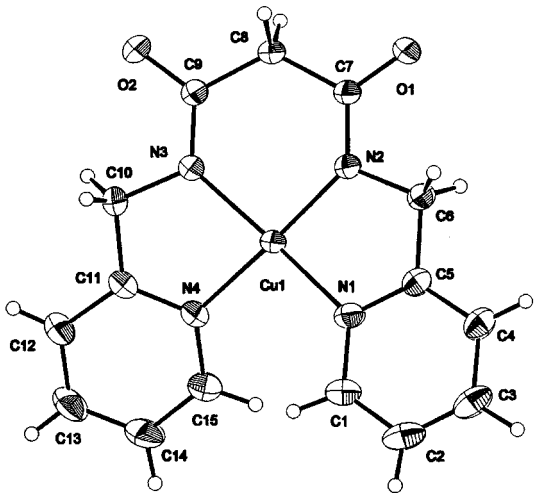

(b)

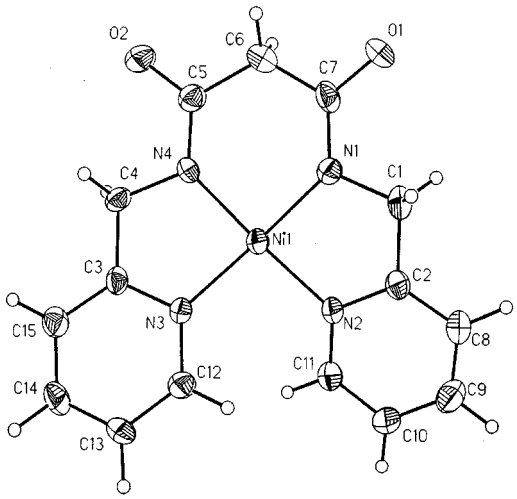

(c)

Table 3. Selected bond lengths (Å) and valence angles (deg) of [M(pap)] (calculated values (MM) in square brackets)

	Cu(II)		Ni(II)		
Cu(1)−N(2)	1.921(2)	[1.92]	1.851(6)	[1.91]	Ni(1)−N(1)
Cu(1)−N(3)	1.927(2)	[1.93]	1.851(6)	[1.91]	Ni(1)−N(4)
Cu(1)−N(4)	2.005(2)	[2.02]	1.909(6)	[1.85]	Ni(1)−N(3)
Cu(1)−N(1)	2.032(2)	[2.02]	1.914(6)	[1.86]	Ni(1)−N(2)
N(2)−Cu(1)−N(3)	94.30(9)	[97.7]	94.2(3)	[90.8]	N(1)−Ni(1)−N(4)
N(2)−Cu(1)−N(4)	173.79(10)	[179.0]	167.6(3)	[178.8]	N(1)−Ni(1)−N(3)
N(3)−Cu(1)−N(4)	82.79(9)	[83.3]	84.7(2)	[88.0]	N(4)−Ni(1)−N(3)
N(2)−Cu(1)−N(1)	82.85(9)	[83.6]	84.0(3)	[87.5]	N(1)−Ni(1)−N(2)
N(3)−Cu(1)−N(1)	163.03(10)	[162.4]	170.0(3)	[164.1]	N(4)−Ni(1)−N(2)
N(4)−Cu(1)−N(1)	101.52(10)	[95.4]	99.1(2)	[93.7]	N(3)−Ni(1)−N(2)

[Ni(pap)]·2H$_2$O: An ORTEP[8] plot of the Ni(II) compound appears in Figure 1c, and the relevant geometric parameters are listed in Table 3. The nickel cation is four-coordinate with a considerable tetrahedral distortion from square-planar geometry [θ = 16.3° (square planar: θ = 0°; tetrahedral: θ° = 90°)]. The Ni−N$_{pyridine}$ and the Ni−N$_{amide}$ distances (1.91 Å and 1.85 Å, respectively) are as expected from comparable chromophores[10]. The tetrahedral distortion is due to the α-hydrogen atoms of the pyridine donor groups (H···H = 2.195 Å), and part of this stress is relaxed by a torsion of the pyridine donor around the Ni−N$_{pyridine}$ axis (14−18°). The five-membered chelate rings are essentially planar.

Molecular Mechanics: The structures of [M(pap)] [M = Co(II), Ni(II), Cu(II), Zn(II)] were computed by strain-energy minimization, using the MOMEC program[11] and force field[12]. All complexes have been modeled as four-coordinate with no axial ligands. So far, MOMEC has mainly been used for five- and six-coordinate transition metal compounds. Metal-ion-related force field parameters are dependent from the coordination geometry[13], i.e. new parameter sets were required for the present study. Also, the approach used in MOMEC for modeling the angular geometry around metal centers is based on 1,3-nonbonded interactions (ligand−ligand repulsion) and, for hexacoordinate compounds, a small perturbation based on the electronic preferences for donor−metal−donor angles of 90°[12b]. For the four-coordinate species considered here, the metal-center-dependent twist from tetrahedral geometry (minimum repulsion) toward square planar coordination was modeled with an out-of-plane term that involves the metal center and the four donor atoms[14]. The force constants and ideal distances for the metal-donor stretching mode and the out-of-plane force constants were fitted to relevant structures available from the Cambridge Structural Data Base (CSD), and five, seven, eight and three sets of X-ray data were used for Co(II), Ni(II), Cu(II) and Zn(II), respectively. The parameters not available before[12] are listed in Table 4. There is good overall agreement between the widely varied experimental data sets and the corresponding computed structures, and the quality of the parameterization with respect to the type of compounds discussed here is demonstrated in Tables 3 and 5, where the computed structural parameters for [Ni(pap)] and [Cu(pap)]

Table 4. Modifications to the published[12] force field

bond stretch	k_b[mdyn Å^{-1}]/r_0 [Å]
Cu−N$_{imine}$	0.600/1.990
Cu−N$_{amide}$	0.600/1.890
Ni−N$_{imine}$	0.600/1.855
Ni−N$_{amide}$	0.600/1.760
Co− N$_{imine}$	0.820/1.960
Co−N$_{amide}$	0.820/1.780
Zn−N$_{imine}$	0.350/2.100
Zn−N$_{amide}$	0.350/2.000

	k_δ[mdyn Å rad^{-2}]			
out-of-plane	Co(II)	Ni(II)	Cu(II)	Zn(II)
M/N$_{amide}$/N$_{imine}$/N$_{amide}$	0.070	0.070	0.050	0.000
M/N$_{amide}$/N$_{amide}$/N$_{imine}$	0.070	0.070	0.050	0.000
M/N$_{imine}$/N$_{imine}$/N$_{amide}$	0.070	0.070	0.050	0.000
M/N$_{imine}$/N$_{amide}$/N$_{amide}$	0.070	0.070	0.050	0.000

Table 5. Comparison of M−N bond distances and tetrahedral twist angles

compound	M−N(amide) [Å] obsd.	calcd.	M−N(pyridine) [Å] obsd.	calcd.	tetrahedral twist angle θ (deg) obsd.	calcd.
[Cu(pap)]	1.92, 1.93	1.92	2.01, 2.03	2.02	18.1	17.7
[Cu(Me$_2$pap)]		1.92		2.01		24.4
[Ni(pap)]	1.85	1.85	1.91	1.91	16.3	15.8
[Ni(Me$_2$pap)]		1.85		1.90		20.0
[Co(pap)]		1.84		1.99		14.5
[Co(Me$_2$pap)]		1.83		1.98		19.6
[Zn(pap)]		1.97		2.08		22.5
[Zn(Me$_2$pap)]		1.96		2.07		31.2

are compared to the experimental data. The geometric parameters of the chromophores of Co(II), Ni(II), Cu(II) and Zn(II), coordinated to pap and Me_2pap are assembled in Table 5, and the calculated structures are presented as SCHAKAL[15] plots in Figure 2.

The computed tetrahedral distortion of [Cu(pap)] and [Ni(pap)] are in good agreement with the experimentally observed twist angles (see Table 5). As expected for a metal ion with d^{10} configuration, the tetrahedral twist of the zinc(II) compound is larger than that of the other com-

Figure 2. SCHAKAL[15] plots of the computed structures of (a) [Co(pap)], (b) [Ni(pap)], (c) [Cu(pap)], (d) [Zn(pap)], (e) [Co(papMe)], (f) [Ni(papMe)], (g) [Cu(papMe)], (h) [Zn(papMe)]

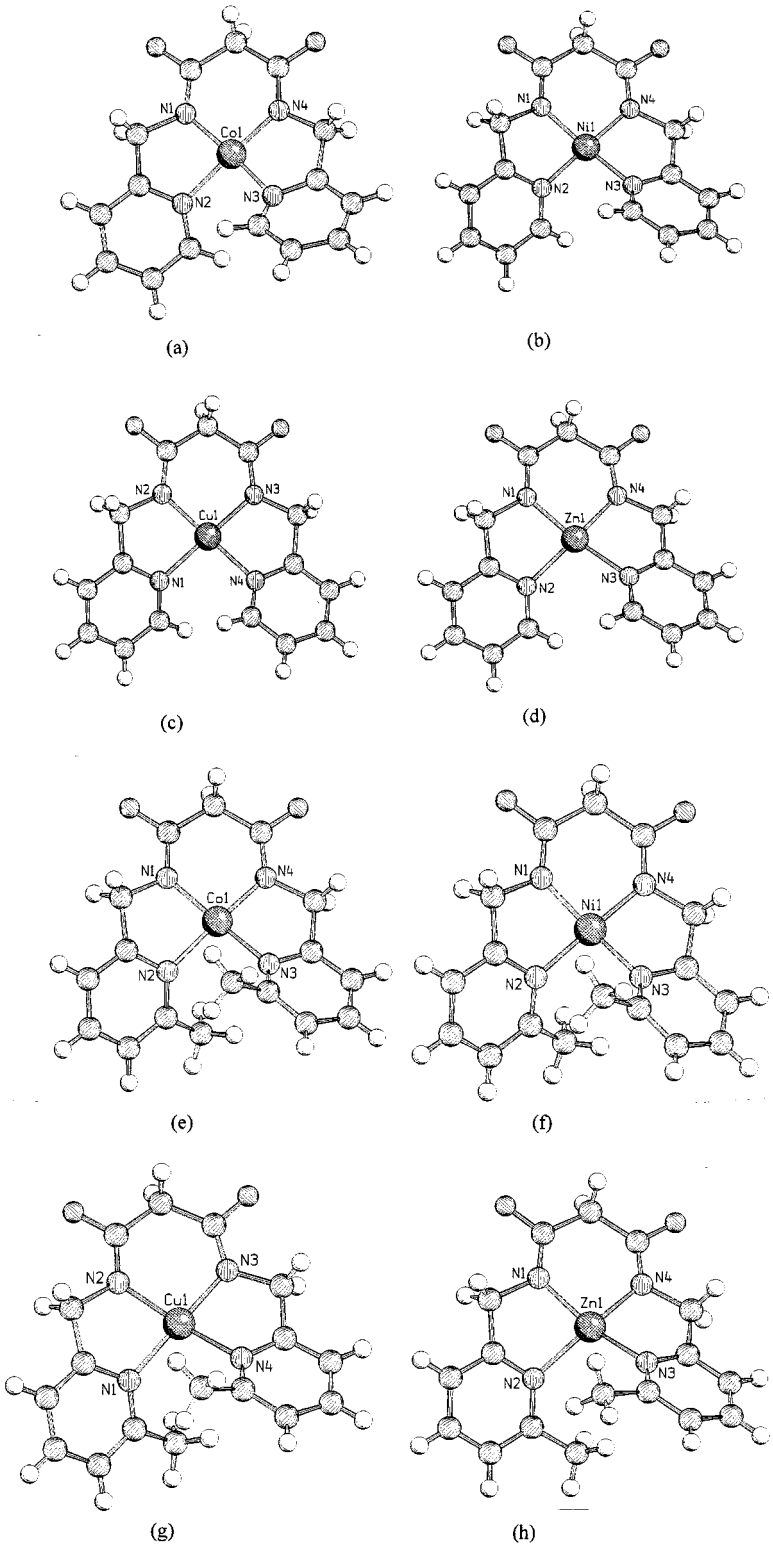

plexes, indicating that Zn(II) may relax the ligand imposed strain most efficiently. Substitution of the ortho hydrogen atoms of the pyridine rings with methyl groups (Me_2papH_2) increases this tetrahedral twist and may thus enhance the zinc(II) selectivity of this type of ligand.

Stabilities

The brutto stability constants of the complexes with $papH_2$ were determined by potentiometric titration [T = 298 K, μ = 0.2 mol dm^{-3} (KCl)]. Table 6 lists the protonation constants of the metal-free ligand and the logβ values of the complex species. The species distribution curves of the Cu(II)/$papH_2$ and the Ni(II)/$papH_2$ systems are shown in Figure 3. The main coordination mode of $papH_2$ with Cu(II) and Ni(II) is through the four nitrogen donors (MLH_{-2} in Figure 3). The supposedly N_2O_2 coordinated compounds [Cu($papH_2$)] and [Ni($papH_2$)] (ML in Figure 3) are minor species in acidic medium, where the amide nitrogen atoms are not deprotonated. The higher stability of [Cu(pap)] than that of [Ni(pap)] is in agreement with the larger flexibility towards tetrahedral distortion (d^9 vs low spin d^8), and this also emerges from the experimentally determined copper(II) selectivity of $C_{16}papH_2$ in the two-phase experiment. From the titration of $papH_2$ in presence of Co(II) and Zn(II) it emerges that [Co($papH_2$)] and [Zn($papH_2$)] are the only complex species present in solution. Thus, this is a good example to demonstrate the limits of computer-assisted design of metal ion selective ligands, i.e. MM does not allow to predict the stoichiometry of the compounds formed in solution[4] (see also Introduction).

Metal-Ion Extraction

$C_{16}papH_2$ is soluble in the most common organic solvents and insoluble in water. The extraction through the liquid membrane (CH_2Cl_2/$C_{16}papH_2$) was studied in two separate experiments, i.e. extraction form the aqueous source phase to the organic phase and extraction form the organic phase to the aqueous receiving phase, and a pH gradient was used to drive the two extraction steps (see Scheme 2). The thermodynamics and kinetics of this type of experiment are dependent on the medium (solvent, pH, ion concentrations), temperature, type of stirring and time for the extraction[16][17]. Also, the stoichiometry of the complex species in the organic phase is not necessarily identical

Figure 3. Species distribution of the M(II)/$papH_2$ system [M(II) = (a) Cu(II), (b) Ni(II); c_M = 2 × 10^{-3} mol dm^{-3}; c_L = 2 × 10^{-3} mol dm^{-3}; μ = 0.2 (KCl)].

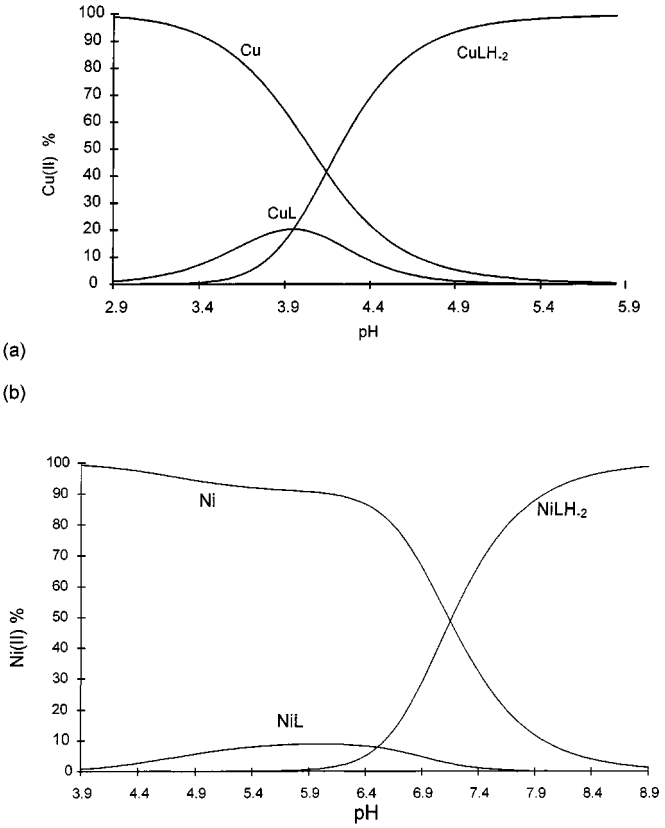

Scheme 2

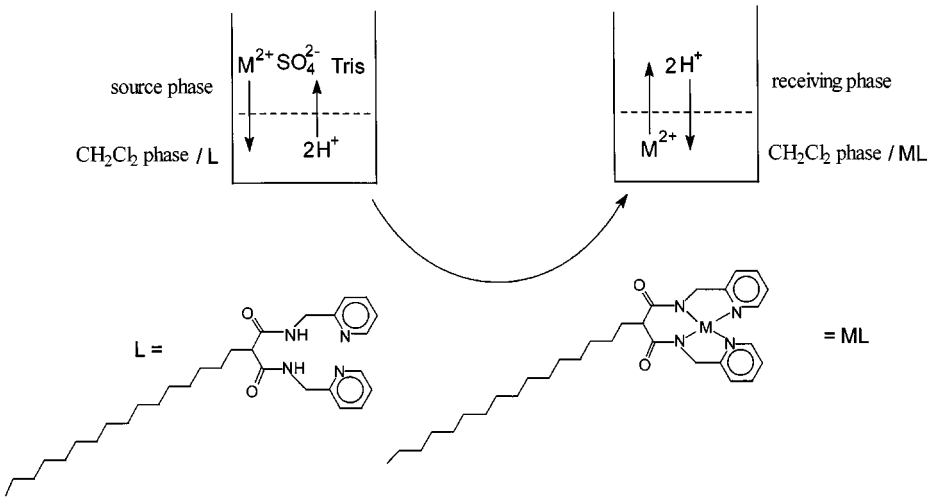

to that in aqueous solution (see comment above). Thus, the extraction data (Table 7) and the results of the potentiometric studies (Table 6) are not comparable on a quantitative basis. Studies in dependence of $[M^{2+}]$ and extraction time indicated that extraction of copper(II) at a relativly low concentration ($[Cu^{2+}] = 5 \times 10^{-3}$ mol dm^{-3}) at ambient temperature and at pH 7.5 (aqueous to organic) and pH 3 (organic to aqueous), respectivly, was complete, i.e. reaching a steady state distribution, after $\leq$ 10 min. At higher $[Cu^{2+}]$ (experiments were performed up to $[Cu^{2+}] =$ 0.02 mol dm^{-3}) the extraction time had to be increased (by a factor of 20 with the above parameters). Also, the extraction kinetics of the four metal ions studied indicate that under the conditions of our experiments, the selectivity for Cu^{2+} was enhanced to some degree. On a qualitative basis the extraction studies and the potentiometric titrations are in good agreement, and the Cu^{2+} selectivity is in agreement with the prediction from the molecular mechanics calculations.

Table 6. Stability constants of the proton, copper(II), nickel(II), cobalt(II) and zinc(II) complexes of $papH_2$ (L)

	metal-free ligand [a]			
log$K$(L)	4.59 (1)			
log$K$(HL^+)	8.48 (1)			
	Co(II)	Ni(II)	Cu(II)	Zn(II)
logβ([MLH_{-2}])		−11.49(2)	−4.49(1)	
logβ([ML])	1.75(1)	1.54(1)	3.41(2)	1.87(1)

[a] $\log K_{amide} = 0.5\ (\log K_{ML} - \log K_{MLH-2})$; Cu(II): 3.95; Ni(II): 6.55

Table 7. $C_{16}papH_2$-mediated extraction of metal ions through CH_2Cl_2 (T = 298 K, pH = 7.5 (source phase), 3 (receiving phase)

source phase	Fe^{2+}	Co^{2+}	Ni^{2+}	Cu^{2+}
$[M^{2+}]_{t\ =\ 0\ min}$ mg/dm^{-3}	25.83	29.50	29.80	27.16
$[M^{2+}]_{t\ =\ 10\ min}$ mg/dm^{-3}	25.38	28.56	27.37	18.12
Extraction[a]	98.3	96.8	91.9	66.7
[%]	(1.7)	(3.2)	(8.2)	(33.3)
Receiving phase	Fe^{2+}	Co^{2+}	Ni^{2+}	Cu^{2+}
$[M^{2+}]_{t\ =\ 10\ min}$ mg/dm^{-3}	0.06	0.13	0.72	8.86
Extraction[b]	13.3	13.8	29.6	98
[%]	(0.2)	(0.4)	(2.4)	(32.6)

[a]% Remaining in source phase (extracted into organic phase). − [b]% Extracted from the organic into the receiving aqueous phase (extracted from aqueous source into aqueous receiving phase).

We gratefully acknowledge generous financial support by the *Deutsche Forschungsgemeinschaft* (*DFG*) and the *Fonds der Chemischen Industrie* (*FCI*).

Experimental Section

General: Commercially available chemicals of the highest possible grade were used without further purification.^{13}C-NMR spectra at 50.32 MHz were obtained with a Bruker AS 200 instrument with sodium 3-(trimethylsilyl)propianate-d_4 as an internal reference. EPR spectra (10^{-3} m in DMF/water (1:2), 298 or 100 K) were recorded with a Bruker ESP 300E instrument (ER 041 XK X-band microwave bridge). The spin-Hamiltonian parameters were determined by simulation of the spectra with the computer program EPR50F[18]. UV/VIS spectra were obtained with Varian Cary IE or Cary 2300 spectrophotometers. Electrochemical measurements (cyclovoltametry) were made with a BAS 100B system using 10^{-3} mol dm^{-3} solutions of [Ni(pap)] in 0.1 mol dm^{-3} tetrabutylammoniumperchlorat CH_3CN solution at a glassy carbon electrode with a Ag/AgCl reference and a Pt auxiliary electrode with a scan rate of 100 mVs^{-1}, or using 10^{-3} mol dm^{-1} solutions of [Cu(pap)] in 0.1 mol dm^{-3} LiCl aqueous solution at a mercury drop electrode with a Ag/AgCl reference and a Pt auxiliary electrode with a scan rate of 100 mVs^{-1}. The pH-metric titrations were performed on 5 or 10 ml samples in the concentration range of 2×10^{-3} to 8×10^{-3} mol dm^{-3} at metal ion to ligand ratios of 2:1, 1:1 and 1:2. Argon was bubbled through the samples to ensure the absence of oxygen and for stirring the solutions. All pH-metric measurements were carried out at 298 K and at a constant ionic strength of 0.2 mol dm^{-3} (KCl). Measurements were made with a Radiometer pHM64 pH-meter, equipped with a CMAWL/S7 combined pH electrode and a Dosimat 715 (Metrohm) autoburette, containing carbonate-free potassium hydroxide at a known concentration. The pH output was converted into $[H^+]$ as described previously[19]. Protonation constants of the ligands and the brutto stability constants of the binary systems were calculated with PSEQUAD[20]. AAS measurements were made on a Perkin-Elmer 1100B instrument using an air-acetylene flame. The spectrometer was calibrated with standard Merck solutions. The wave lengths: 324.7 nm (Cu), 232 nm (Ni), 240.7 nm (Co), 248.3 nm (Fe). Elemental analyses were obtained from the microanalytical laboratory of the chemical institutes of the University of Heidelberg.

For molecular mechanics calculations MOMEC[11] was used, which also produced the Schakal[15] files for plotting. The force field has been described previously[11], except for parameters that are described in the text and in Table 4.

$papH_2$: α-picolylamine (2.7 g, 25 mmol) was added slowly to a hot and stirred aqueous solution (100 ml, 100°C) of diethyl-malonate (16 g, 6.25 mmol), and left at this temperature for 8h. After cooling to ambient temperature, ethanol (10 ml) and ether (100 ml) were added to precipitate the yellowish white product, which was collected after 24h (refrigerator) and recrystallized from ethyl acetate. Yield of the white crystalline ligand: 25.56 g (89.9 mmol, 90%). Calcd. for $C_{15}H_{16}N_4O_2$: C 63.35, H 5.68, N 19.71; found: C 63.29, H 5.73, N 19.78. ^{13}C-NMR (50.32 MHz, CD_3OD, 25°C, TMS): 169.7 (CO), 158.9, 149.7, 138.8, 123.7, 122.9 ($C_{pyridine}$), 53.8 ($CH_2(CO)_2$), 45.5 (pyridine, CH_2-NHR).

$C_{16}papH_2$: Diethyl malonate (8 g, 50 mmol) was slowly added by syringe to a solution of sodium (1.15 g, 50 mmol) in warm ethanol (abs., 25 ml, 50°C). Upon slow addition (syringe) of hexadecyl bromide (15.5 g, 50.25 mmol), a white product precipitate. The reaction mixture was then refluxed for 6 h and left in a refrigerator for 12 h. The precipitated diethyl hexadecylmalonate was collected by filtration, washed with water and dried over P_2O_5. Yield: 16.7 g (43.4 mmol, 87%). Calcd. for $C_{23}H_{44}O_4$: C 71.81, H 11.54; found: C 72.01, H 11.63. ^{13}C NMR (50.32 MHz, $CDCl_3$, 25°C, TMS): δ = 169.6 (CO), 61.2 (CH_2, ester), 52.1 ($C_{16}-CH-R_2$), 14.1 (CH_3, ester), mult (alkyl chain).

α-Picolylamine (18 g, 166.4 mmol) and the alkylated diethyl malonate (16 g, 41.6 mmol) were allowed to react for 8 h at 100°C

Table 8. Crystal data

	papH$_2$ × HBF$_4$ × H$_2$O	[Ni(pap)] × 2 H$_2$O	[Cu(pap)] × 3 H$_2$O
formula	$C_{15}H_{19}N_4O_3BF_4$	$C_{15}H_{14}N_4O_2Ni \times 2\ H_2O$	$C_{15}H_{14}N_4O_2Cu \times 3\ H_2O$
crystal system	orthorhombic	triclinic	monoclinic
Mol. mass	390.14	377.02	399.89
space group	*Pnma*	*Ci*/1,*P*1bar	$P2_1/a$
a [Å]	8.700(2)	7.794 (2)	8.0810(10)
b [Å]	13.145(3)	11.933 (4)	22.086(3)
c [Å]	15.401(4)	17.808 (5)	9.9390(10)
α [°]	90	86.83 (3)	90
β [°]	90	82.70 (2)	104.520(10)
γ [°]	90	73.82 (2)	90
V [Å^3]	1761.28	1577.1	1717.2
Z	8	2	4
Crystal colour, habit	light green prisms	red plates	blue plates
Crystal dimensions [mm]	0.50 × 0.55 × 0.65	0.10 × 0.35 × 0.50	0.55 × 0.50 × 0.35
Radiation [mm^{-1}]	Mo-K_α, μ = 0.13	Mo-K_α, μ = 1.26	Mo-K_α, μ = 1.306
θ limits [deg]	1.5 < θ < 29.5	1.5 < θ < 25.0	1.84 < θ < 30.0
$D_{calcd.}$ [g/cm^3]	1.47	1.59	1.547
No. of unique reflections	2539	5553	5174
No. of independent reflections	1643	3269	4938
temp.,°C	22	22	22
λ [Å]	0.7101	0.7101	0.7101
R	0.084	0.061	0.047
R_w [a]	0.069	0.050	0.1017

[a] $R_w = \Sigma w(|F_o| - |F_c|^2.\Sigma w F_o^2)^{1/2}$.

without a solvent. The product mixture was poured into 50 ml of cold water, and the precipitate was collected on a filter, after standing for 4 h in the refrigerator. After washing with water and drying under reduced pressure, the diamide was recrystallized from dichloromethane. Yield: 14.82 g (29.13 mmol, 70%). Calcd. for $C_{31}H_{48}N_4O_2$: C 73.17, H 9.52, N 11.02; found: C 72.99, H 9.47, N 10.95. ^{13}C NMR (50.32 MHz, $CDCl_3$, 25°C, TMS): δ = 170.8 (CO), 156.4, 149.1, 136.6, 122.2, 121.6 ($C_{pyridine}$), 55.2 ($C_{16}-CH-(CO)_2$), 44.6 (pyridine, CH_2-NHR), mult (alkyl chain).

[Cu(pap)]: An aqueous solution (30 ml) of $CuSO_4 \times 5\ H_2O$ (0.44 g, 1.76 mmol) was added to an aqueous solution (30 ml) of papH$_2$ (0.5 g, 1.76 mmol), set at pH 7.5 (0.1 M aqueous NaOH). A crystalline product was obtained after slow evaporation of the solvent at ambient temperature. Yield: 0.57 g (1.43 mmol, 81.4%). Calcd. for $C_{15}H_{20}CuN_4O_5$: C 45.05, H 5.04, N 14.01; found: C 44.99, H 5.07, N 14.04.

[Ni(pap)]: An aqueous solution (30 ml) of $Ni(BF_4)_2$ (0.41 g, 1.76 mmol) was added to an aqueous solution (30 ml) of papH$_2$ (0.5 g, 1.76 mmol), set at pH 7.5 (0.1 M aqueous NaOH). A crystalline product was obtained after slow evaporation of the solvent at ambient temperature. Yield: 0.42 g (1.11 mmol, 63.6%). Calcd. for $C_{15}H_{18}N_4NiO_4$: C 47.79, H 4.81, N 14.86; found: C 47.52, H 4.80, N 14.83. ^{13}C NMR (50 MHz, CD_3OD, 25°C, TMS): 176.2 (CO), 165.7, 150.6, 140.7, 125.7, 123.0 ($C_{pyridine}$), 57.6 ($CH_2(CO)_2$), 44.9 (pyridine, CH_2-NR).

Crystal Structure Analyses: The X-ray data of papH$_2$ × HBF$_4$ × H$_2$O ($C_{15}H_{19}N_4O_3 \times BF_4$), [Ni(pap)] × 2 H$_2$O ($C_{15}H_{14}N_4O_2Ni \times 2\ H_2O$) and [Cu(pap)] × 3 H$_2$O ($C_{15}H_{14}CuN_4O_2 \times 3\ H_2O$) were measured at room temperature on a Nicolet R3-diffractometer employing graphite monochromated Mo-K_α radiation (λ = 0.7107 Å); ω scan mode, data reduction and application of Lorenz, polarization absorption corrections were carried out. Details of the measurements and analyses are given in Table 8. The atom numbering is defined in Figure 1. The crystallographic data have been deposited at the Cambridge Crystallographic Data Centre (CCDC) as supplementary publication no. CCDC-103064 (for $C_{15}H_{14}N_4O_2Ni \cdot 2H_2O$), -103065 (for $C_{15}H_{19}N_4O_3BF_4$), -103066 (for $C_{15}H_{14}N_4O_2Cu \cdot 3H_2O$). Copies of the data can be obtained free of charge on application to CCDC, 12 Union Road Cambridge CB2 1EZ, UK [Fax: (internat.) + 44-1223/336033; E-mail: deposit@ccdc.cam.ac.uk].

The structure of papH$_2$ × HBF$_4$ × H$_2$O was solved with direct methods; full-matrix least-squares methods were used to refine 2790 variables out of 1643 reflections with $I > 2.5\sigma$ (I); the structure converged at R = 8.4% and R_W = 6.9%; residual electron density −0.42, 0.71 e/Å^{-3}. Weight = $1/\sigma^2(F_0)$; goodness of fit = 4.19. The structures [Ni(pap)] × 2 H$_2$O and [Cu(pap)] × 3 H$_2$O were solved by Patterson-Fourier Methods with the SHELXTL PLUS program[21]; hydrogen atoms were included at calculated sites with fixed isotropic thermal parameters. The refinement (full-matrix, least-squares methods, $|F|$) of 5553 ([Ni(pap)]), 5174 ([Cu(pap)]) variables out of 3269 ([Ni(pap)]), 4938 ([Cu(pap)]) reflections with $I > 2.5\sigma$ (I) converged at R = 6.1% ([Ni(pap)]), 4.7% ([Cu(pap)]) and R_W = 5.0% ([Ni(pap)]), 10.17% ([Cu(pap)]); residual electron density −0.45, 0.54 ([Ni(pap)]), −0.327, 0.522 e/Å^{-3} ([Cu(pap)]). Weight = $1/\sigma^2(F_0)$; goodness of fit = 1.91 ([Ni(pap)]), 1.092 ([Cu(pap)]).

Extraction Experiments: The volume of each phase (aqueous source phase, organic phase, aqueous receiving phase) was 50 ml. The M^{2+} concentration (M = Fe, Co, Ni, Cu) of the aqueous source phase was ca. 5 × 10^{-3} mol dm^{-3} (pH 7.5, 0.1 mol dm^{-3} Tris, filtration to remove hydroxides) and measured by AAS (1 ml samples). The organic phase (CH_2Cl_2) contained 10^{-3} mol dm^{-3} C_{16}papH$_2$ and the pH of the aqueous receiving phase was 3 (0.1 mol dm^{-3} phthalate). The extractabilities were determined by AAS as decreasing [M^{2+}] in the aqueous source and increasing [M^{2+}] in the aqueous receiving phase. The conditions for all extractions were identical (298 K, stirring at 750 r.p.m. (magnetic stirrer) for 10.0 min). The data reported in Table 7 are averages of 3 determinations (deviation ≤ 5%).

[1] [1a] H. Irving, R. J. P. Williams, *Nature (London)* **1948**, *162*,

746. – [1b] D. A. Johnson, P. G. Nelson, *Inorg. Chem.* **1995**, *34*, 5666. – [1c] D. A. Johnson, P. G. Nelson, *J. Chem. Soc., Dalton Trans.* **1995**, 3483.
[2] D. J. Cram, T. Kaneda, R. C. Helgeson, S. B. Brown, C. B. Knobler, E. Maverick, K. N. Trueblood, *J. Am. Chem. Soc.* **1985**, *107*, 3645.
[3] [3a] R. D. Hancock, *Progr. Inorg. Chem.* **1989**, *37*, 187. – [3b] A. E. Martell, R. D. Hancock, *"Metal complexes in Aqueous Solution"*, Plenum, New York, **1996**. – [3c] L. F. Lindoy, *"The Chemistry of Macrocyclic Ligand Complexes"*, Cambridge University Press, Cambridge, **1989**. – [3d] K. R. Adam, L. F. Lindoy, in *"Crown Compounds, Toward Future Applications"*, Ed. S. R. Cooper, VCH, Weinheim, **1992**, p.69.
[4] [4a] P. Comba, T. W. Hambley, *"Molecular Modeling of Inorganic Compounds"*, VCH, Weinheim, **1995**. – [4b] P. Comba, *Coord. Chem. Rev.*, **1998**, *submitted*.
[5] [5a] P. Comba, A. Fath, A. Kühner, B. Nuber, *J. Chem. Soc., Dalton Trans.*, **1997**, 1889. – [5b] P. Comba, B. Nuber, A. Ramlow, *J. Chem. Soc., Dalton Trans.*, **1997**, 347. – [5c] B. P. Hay, D. Zang, J. R. Rustad, *Inorg. Chem.*, **1996**, *35*, 2650. – [5d] P. Comba, K. Gloe, K. Inoue, T. Krueger, H. Stephan, K. Yoshizuka, *Inorg. Chem.* **1998**, *37*, 3310. – [5e] P. Comba, N. Okon, R. Remenyi, *Chem. Europ. J.* **1998**, *submitted*.
[6] K. Várnagy, H. Süli-Vargha, in *"Molecular Modeling and Dynamics of Bioinorganic Systems"*, Eds. L. Banci, P. Comba, Kluwer, Dordrecht, **1997**.
[7] P. Comba, T. W. Hambley, G. A. Lawrance, *Helv. Chim. Acta* **1985**, *68*, 2332.
[8] C. K. Johnson, *ORTEP*; Report 3794; U.S. Atomic Energy Commission, Oak Ridge: TN, **1965**.
[9] [9a] S. Tsuboyama, T. Sakurai, K. Kobayashi, *Acta Cryst.*, **1984**, *40*, 466. – [9b] R. L. Chapman, F. S. Stephens, R. S. Vagg, *Inorg. Chim. Acta* **1980**, *43*, 29. – [9c] M. Mulqi, F. S. Stephens, R. S. Vagg, *Inorg. Chim. Acta* **1981**, *51*, 9. – [9d] F. S. Stephens, R. S. Vagg, *Inorg. Chim. Acta*, **1981**, *51*, 149. – [9e] M. Mulqi, F. S. Stephens, R. S. Vagg, *Inorg. Chim. Acta* **1981**, *52*, 177. – [9f] R. L. Chapman, F. S. Stephens, R. S. Vagg, *Inorg. Chim. Acta* **1981**, *52*, 169. – [9g] M. Ray, R. Mukherjee, J. F. Richardson, M. S. Mashuta, R. M. Buchanan, *J. Chem. Soc. Dalton Trans.* **1994**, 965.
[10] [10a] M. Mulqi, F.S. Stephens, R.S. Vagg, *Inorg. Chim. Acta*, **1981**, *52*, 73. – [10b] S. C. Chang, D. Y. Park, N. C. Li, *Inorg. Chem.* **1968**, *7*, 2144. – [10c] F. S. Stephens, R. S. Vagg *Inorg. Chim. Acta*, **1984**, *90*, 17. – [10d] F. S. Stephens, R. S. Vagg, *Inorg. Chim. Acta*, **1986,** *120*, 165. – [10e] F. S. Stephens, R. S. Vagg, *Inorg. Chim. Acta*, **1982**, 57, 9.
[11] P. Comba, T. W. Hambley, N. Okon, G. Lauer, *"MOMEC, a Molecular Modeling Package for Inorganic Compounds"*, **1997**, Lauer & Okon, Heidelberg, Germany, E-mail: CVS-HD@t-online.de.
[12] [12a] P. V. Bernhardt, P. Comba, *Inorg. Chem.* **1992**, *31*, 2638. – [12b] P. Comba, T. W. Hambley, M. Ströhle, *Helv. Chim. Acta* **1995**, *78*, 2042. – [12c] J. E. Bol, C. Buning, P. Comba, J. Reedijk, M. Ströhle, *J. Comput. Chem.* **1998**, *19*, 512.
[13] P. Comba in *"Fundamental Principles of Molecular Modeling"*, A. Amann, J. C. A. Boeyens, W. Gans, Eds., Plenum Press, New York, **1996**, 167.
[14] The new version of the program MOMEC[11] has a plane twist potential to model tetrahedral twists; this facility was not used in the present study.
[15] E. Keller, *SCHAKAL 92*, Universität Freiburg, Germany, **1992**.
[16] E. Kimura, C. A. Dalimunte, A. Yamashita, R. Machida, *J. Chem. Soc., Chem. Comm.*, **1985**, 1041.
[17] M. DiCasa, L. Fabbrizzi, A. Perotti, A. Poggi, P. Tundo, *Inorg. Chem.*, **1985**, *24*, 1610.
[18] P. A. Martinelli, G. R. Hanson, J. S. Thompson, B. Holmquist, J. R. Pilbrow, B. L. Vallee, *Biochemistry* **1980**, *28*, 225.
[19] [19a] A. Gergely, I. Nagypal, *J. Chem. Soc., Dalton Trans.* **1977**, 104. – [19b] H. M. Irving, M. H. Miles, L. D. Pettit, *Anal. Chim. Acta*, **1967**, *38*, 475.
[20] L. Zékány, I. Nagypál in: *"Computational methods for the Determination of Stability Constants"*, ed. D. Leggett, Plenum Press, **1985**.
[21] G. M. Sheldrick, Universität Göttingen, SHELXTL PLUS, Release 4.11 (V), **1990**.

[I98226]